

REPORT DOCUMENTATION PAGE

AD-A255 968

2

1a. REPORT SECURITY CLASSIFICATION UNCLASSIFIED			1b. RESTRICTIVE NONE		
2a. SECURITY CLASSIFICATION AUTHORITY			3. DISTRIBUTION Approved for public release: Distribution unlimited		
2b. DECLASSIFICATION/DOWNGRADING SCHEDULE OCT 07 1992					
4. PERFORMING ORGANIZATION REPORT NUMBER ONR 39			5. MONITORING ORGANIZATION REPORT NUMBER(S) AFOSR-TR-82-0867		
6a. NAME OF PERFORMING ORGANIZATION University of California, Santa Barbara		6b. OFFICE SYMBOL (If applicable)		7a. NAME OF MONITORING ORGANIZATION Air Force Office of Scientific Research	
6c. ADDRESS (City, State, and ZIP Code) Santa Barbara, California 93106-5090			7b. ADDRESS (City, State, and ZIP Code) Building 410 Bolling Air Force Base, DC 20332-6448		
8a. NAME OF FUNDING/SPONSORING ORGANIZATION Air Force Office of Scientific Research (AFOSR)		8b. OFFICE SYMBOL (If applicable) NC		9. PROCUREMENT INSTRUMENT IDENTIFICATION NUMBER AF49620-88-0138	
8c. ADDRESS (City, State, and ZIP Code) Building 410 Bolling Air Force Base, DC 20332-6448			10. SOURCE OF FUNDING NUMBERS		
			PROGRAM ELEMENT NO 61102 F	PROJECT NO. 2303	TASK NO. A3
11. TITLE (Include Security Classification) Oriented Electro/Optical Polymers through In-Situ Chemistry during Gel Processing: A Research Opportunity					
12. PERSONAL AUTHOR(S) Alan J. Heeger					
13a. TYPE OF REPORT Final Report		13b. TIME COVERED FROM 09/15/88 to 12/31/90		14. DATE OF REPORT (Year, Month, Day) September 4, 1992	
15. PAGE COUNT 12					
16. SUPPLEMENTARY NOTATION					
17. COSATI CODES			18. SUBJECT TERMS (Continue on reverse if necessary and identify by block number)		
FIELD	GROUP	SUB-GROUP			
19. ABSTRACT (Continue on reverse if necessary and identify by block number)					
<p>The focus of the research was to obtain high performance properties (electrical and/or optical) from conjugated polymers by improving the structural order through polymer processing. The success of the approach is quantified by the demonstration of third order optical susceptibility values in excess of 10^{-8}-10^{-7} esu for high quality, oriented <i>trans</i>-polyacetylene at frequencies in the infrared (frequencies which are relevant to optical communications). Equally important, we have identified a structure/property relationship that can be used to direct synthesis of new conjugated polymers with comparably large NLO coefficients: In conjugated polymers with degenerate ground state, the dominant NLO mechanism results from the neutral soliton A_g intermediate state mechanism. In a parallel effort, high performance electrical and mechanical properties were demonstrated in fibers made from conducting polymers.</p>					
20. DISTRIBUTION/AVAILABILITY OF ABSTRACT <input checked="" type="checkbox"/> UNCLASSIFIED/UNLIMITED <input type="checkbox"/> SAME AS RPT <input type="checkbox"/> DTIC USERS			21. ABSTRACT SECURITY CLASSIFICATION UNCLASSIFIED		
22a. NAME OF RESPONSIBLE INDIVIDUAL De Charles Lee			22b. TELEPHONE (Include Area Code) (202) 767-49		22c. OFFICE SYMBOL AFOSR/NC

Final Technical Report
to
Air Force Office of Scientific Research (AFOSR)
Bolling Air Force Base, DC
Attention: Dr. Charles Lee, Program Officer

**Oriented Electro/Optical Polymers Through *In-Situ*
Chemistry During Gel Processing:
A Research Opportunity**

AFOSR Contract #F49620-88-C-0138

Institute for Polymers and Organic Solids
University of California, Santa Barbara
Santa Barbara, California 93106

92 10 0 068

414397
92-26587 1/8
235


Principal Investigators:

Professor Alan J. Heeger

Telephone: (805) 893-3184
FAX: (805) 893-4755

Professor Paul Smith

Telephone: (805) 893-8104
FAX: (805) 893-4755

Professor Fred Wudl

Telephone: (805) 893-3755
FAX: (805) 893-4755

Approved for public release ;
distribution unlimited.

I. Introduction

In conjugated polymers, charge injection is followed by structural relaxation to form self-localized nonlinear excitations; solitons, polarons and bipolarons.¹ For example in *trans*-polyacetylene, solitons are formed by n- or p-type charge injection through chemical or electrochemical doping, by n- or p-type charge injection at an MIS interface, or by electron-hole pair injection (with subsequent charge separation) through photo-excitation at $\hbar\omega > E_g$ where $E_g = 2\Delta$ is the energy gap and Δ is the order parameter of the bond-alternating ground state. In each case, experiments have demonstrated a structural deformation and an associated electronic state near mid-gap, with a corresponding shift in oscillator strength. Time-resolved measurements have shown that this shift in oscillator strength occurs on the sub-picosecond time scale as predicted by Su and Schrieffer. These shifts in oscillator strength following photo-absorption cause relatively large changes in optical constants, and hence provide a mechanism for the large resonant third order susceptibility.²

The connection between the nonresonant nonlinear optical (NLO) response to optical pumping well below the absorption edge and the resonant NLO response following absorption and photo-excitation has been discussed in terms of contributions from virtual soliton pairs enabled by nonlinear zero-point fluctuations in the ground state. Because of the nonlinear zero-point motion, there are finite matrix elements connecting the ground state with the relaxed state following the creation of a soliton-antisoliton ($S-\bar{S}$) pair. This mechanism implies a sensitivity of $\chi^{(3)}$ to the existence of a degenerate ground state; lifting the degeneracy would confine the $S-\bar{S}$ pair, inhibit separation, and thereby limit the NLO response.

Standard third-order perturbation theory yields the following expression for $\chi^{(3)}(3\omega)^3$:

$$\chi^{(3)}(3\omega) = e^4 \sum_m \sum_n \sum_p [f_{gn} f_{nm} f_{mp} f_{pg}] \{ [E_{mg} - 3\hbar\omega][E_{ng} - 2\hbar\omega][E_{pg} + 3\hbar\omega] \}^{-1} + \dots \quad (1)$$

where f_{gn} represents the dipole matrix element between the ground state (g) and an excited state (n, m, or p), and E_{ng} represents the $g \rightarrow n$ energy difference (and E_{mg} represents the $g \rightarrow m$ energy

<input checked="checked" type="checkbox"/>	
<input type="checkbox"/>	
<input type="checkbox"/>	
Code	
/or	
Dist	Special
A-1	

DTIC QUALITY INSPECTED 1

difference, etc). Since the ground state has A_g symmetry, the dipole matrix elements require the following sequence of virtual transitions:

$$g \rightarrow n (B_u \text{ symmetry}) \rightarrow m (A_g \text{ symmetry}) \rightarrow p (B_u \text{ symmetry}) \rightarrow g.$$

Since the strongest matrix elements for dipole transitions from the ground state to excited states at relatively low energy are to the excited states with an electron and a hole in states with wave vector k in the valence and conduction bands respectively (the kB_u states), *the challenge is to find the A_g state with the largest transition dipole moment starting from the kB_u states.*

We have discovered⁴ that the virtual transition from the kB_u state to the A_g state consisting of a pair of neutral solitons has two unique and critically important features:

- (i) The matrix element contains an enormous enhancement factor, $\pi^4(\xi_0/a)^2$, where $\xi_0/a \approx 7$ is the half width of the soliton in units of the carbon-carbon distance along the chain. This enhancement factor can be traced back directly to the remarkable strength of the soliton mid-gap transition;
- (ii) The energy to create a separated soliton pair is¹ $E_{S-S} = (2/\pi)E_g$; consequently, Eqn. 1 can be *simultaneously* resonant for three-photon and two-photon processes for a single pump frequency:

$$3\omega \rightarrow E_g,$$

$$2\omega \rightarrow (2/\pi)E_g$$

As a result, for conducting polymers with a degenerate ground state, the magnitude of $\chi^{(3)}(-3\omega; \omega, \omega, \omega)$ will be significantly enhanced by the virtual soliton mechanism.

Since confinement by resonance structures with different energies eliminates the free, separated soliton pair states, lifting the degeneracy will quench this NLO mechanism, emphasizing the importance of the interconnection between the chemical structure and the electronic properties of conducting polymers.

We have recently reported⁶ (see following Section) the initial results of THG measurements on *cis*- and *trans*-polyacetylene over the pump frequency range from 0.55 eV through 1.25 eV (see following Section). The results show that $\chi^{(3)}(-3\omega;\omega,\omega,\omega)$ for *trans*-polyacetylene is an order of magnitude larger than that for the *cis*-isomer over the entire spectral range, even comparing the respective 3ω resonance maxima.

The THG data, therefore, prove the existence of a symmetry specific NLO mechanism favoring the degenerate ground state system, consistent with an important contribution from virtual soliton pairs enabled by nonlinear zero-point fluctuations. These experimental results and the progress in theory that were stimulated by the results demonstrate that peak values for $\chi^{(3)}$ of order 10^{-7} esu should be achievable for a conjugated polymer with a degenerate ground state, and that an enhancement of $\chi^{(3)}$ by more than an order of magnitude over the rigid band contribution due to the (S-S) A_g intermediate state contribution can be expected for a system with a degenerate ground state.

II. Detailed Summary of Significant Results

We summarize experimental results which demonstrate the existence of a mechanism for NLO response which is specific to the degenerate ground state polymer. Comparative THG measurements on *cis*- and *trans*-(CH)_x over the pump frequency range 0.55eV-1.3 eV show that $\chi^{(3)}$ for *trans*-(CH)_x is an order of magnitude larger over the entire spectral range.^{6,7} The data imply an important contribution to $\chi^{(3)}$ from virtual soliton pairs enabled by nonlinear zero-point fluctuations.

Although the *cis/trans* comparison is consistent with the soliton pair intermediate A_g state mechanism, the measured $\chi^{(3)}(3\omega)$ values obtained from as-grown polyacetylene films are more than an order of magnitude smaller than calculated. To achieve the predicted high performance values for $\chi^{(3)}(3\omega)$, materials of the highest quality are required; oriented *trans*-(CH)_x with structural order sufficient to obtain an electrical conductivity (after doping) of ~20,000 S/cm. The reduced disorder increases $\chi^{(3)}(3\omega)$ by more than an order of magnitude to 10^{-8} - 10^{-7} esu for $\hbar\omega$ within the energy gap (E_g), in agreement with the calculated contribution from $S\bar{S}$ intermediate states.

A. $\chi^{(3)}(3\omega)$ Measurements of *cis*- and *trans*-(CH)_x: Symmetry Specific NLO Mechanism

For the *cis-trans* comparison experiment, thin film *cis*-(CH)_x was synthesized using the Shirakawa method⁸ onto a sapphire substrate which was mounted onto a cold finger; to prevent conversion to the *trans*-isomer, the cold finger was maintained at 195K using a dry ice/acetone mixture. After completing the THG measurements on the *cis*-isomer, conversion to *trans*-(CH)_x was accomplished by heating the sample to 438K; to minimize errors, the *same sample* was used for both the *cis*- and *trans*-(CH)_x THG measurements. Absorption spectra taken before and after each series of measurements showed that conversion from *cis*- to *trans*-(CH)_x was not induced by beam heating (or other causes) during the measurements

THG measurements were referenced to a fused silica plate of known $\chi^{(3)}$ and index of refraction.^{9a,9b} The light source was a Nd:YAG laser; the frequency doubled output pumped a dye laser, which in turn pumped either a Raman shifter or a difference frequency generator. The fundamental (ω) was tuneable from 0.55 eV to 1.4 eV. The Maker's fringe method was used¹⁰; THG intensity measurements were taken at 31 different angles using a rotation stage. To improve the signal to noise ratio, each point on the fringe pattern was an average of 128 measurements of THG intensity waveform. Since each data point requires two Maker's fringe measurements (on the sample and on the reference), each $\chi^{(3)}(3\omega)$ is based on 7936 measurements of THG intensity. The $\chi^{(3)}(3\omega)$ values were reproducible within 15%, including variations across the sample.

The data, $\chi^{(3)}(-3\omega; \omega, \omega, \omega)$ vs ω are summarized in Figure 1; solid points are for *trans*-(CH)_x and open circles are for "cis"-(CH)_x; i.e *cis*-(CH)_x containing about 10-15% of the *trans*-isomer. Since it is difficult to obtain pure *cis*-(CH)_x, the solid curves represent the data analyzed in terms of effective medium theory:

$$\chi^{(3)}(3\omega) = (1-f) \chi^{(3)}(3\omega)|_{\text{cis}} + f \chi^{(3)}(3\omega)|_{\text{trans}} \quad (2)$$

where f is the volume fraction of *trans*-(CH)_x in the "cis"-(CH)_x. In Eqn 2, $\chi^{(3)}(3\omega)$ is assumed to be of the form obtained from perturbation theory (see Eqn 1).³ Implicit in the effective medium theory is the assumption that the *cis* and *trans* regions in the partially isomerized sample occur at random on a length scale smaller than the wavelength of the light so that one must add before squaring to get the output power. The implied interference is evident in the anti-resonance observed at 0.65eV in the *cis*-(CH)_x data; the solid curve is the fit to Eqn 1 with $f = 0.11$. The $\chi^{(3)}(3\omega)$ values from different samples were in good agreement; the data in Fig. 1 represent an average from two independently prepared samples.

The results in Figure 1 demonstrate that the nonresonant values of $\chi^{(3)}(3\omega)|_{\text{trans}}$ (dot-dashed curve) are 10-20 larger than $\chi^{(3)}(3\omega)|_{\text{cis}}$ (dashed curve) over the entire spectral range.⁵ On resonance, where the peak value is inversely proportional to the linewidth, the peak value for *trans*-(CH)_x is still five times larger, even though the *cis*-(CH)_x three-photon resonance is an order of magnitude narrower. The *trans-cis* $\chi^{(3)}$ -ratio is, therefore, significantly larger than that predicted in the rigid lattice approximation,² where any difference in $\chi^{(3)}(3\omega)$ between the two isomers would be proportional to E_g^{-6} .

We conclude that there exists an important contribution to $\chi^{(3)}(3\omega)$ which is symmetry specific, favoring the degenerate ground state.

B. The Role of Disorder

The larger values of $\chi^{(3)}$ for *trans*-(CH)_x (Fig. 1) can be qualitatively understood if we consider the rigid band contribution to be characteristic of *cis*-(CH)_x where the ground state degeneracy has been lifted, and the soliton pair excitations confined. However, the absolute value

of $\chi^{(3)}(3\omega)_{\text{trans}}$ is an order of magnitude smaller than the calculated curves⁴ at all frequencies. We have shown that this discrepancy arises from disorder-induced localization of the π -electron wavefunctions on the polyene chains.

It is well-known that disorder causes localization of electronic wavefunctions in one-dimensional systems. In general, the mean localization length, l_{loc} , is limited by structural order; $l_{\text{loc}} \leq l_p \leq L$ where l_p is the persistence length, and $L = Na$ is the end-to-end chain length. A dramatic increase in NLO response with increasing conjugation length has been predicted;^{11,12} $\chi^{(3)}/n \sim n^v$ where n is the polymerization index, and $v \approx 3-4$. Although $\chi^{(3)}/n$ must saturate for long chains, saturation does not occur¹² until $n \sim 10^2$.

Because of disorder, l_{loc} can be expected to be much less than L , thus limiting $\chi^{(3)}$. Since disorder-induced localization limits the electrical conductivity, σ , in all but the most highly ordered samples of doped conducting polymers,¹³ one can estimate l_{loc} from the mean free path (λ) inferred from the conductivity. For $\sigma = 10^4$ S/cm, $\lambda \sim 100$ Å while for $\sigma < 10^2$ S/cm all states are localized with λ at most a few lattice constants. The implied short conjugation length for typical polymers implies that ordered macromolecules are required to obtain the anticipated advantages of delocalization on $\chi^{(3)}$.

In Figure 2, we plot $\chi^{(3)}_{\parallel}(3\omega)$ for an oriented sample of *trans*-(CH)_x (draw ratio 10) prepared using the best techniques currently available¹⁴; the subscript denotes the diagonal component; both the ω and 3ω beams are polarized parallel to the orientation direction. Such samples, when doped with Iodine routinely yield $\sigma \sim (1-3) \times 10^4$ S/cm.¹⁴ The spectrum is essentially identical to that in Figure 1, but the magnitude of $\chi^{(3)}$ has increased by more than an order of magnitude (a factor of 40 near the simultaneous two and three-photon resonance). Since the orientational average for a random sample is $\langle \cos^6 \theta \rangle^{1/2} = (1/7)^{1/2}$, the large increase in $\chi^{(3)}_{\parallel}(3\omega)$ results primarily from π -electron delocalization.

C. Comparison of the Results with the Soliton A_g Intermediate State NLO Mechanism

Since solitons are known to be important nonlinear excitations in *trans*-(CH) $_x$, and since the energy to form a separated $S\bar{S}$ pair is less than E_g ,¹ $S\bar{S}$ pairs might be expected to be important intermediate states in Eqn. 2. Moreover, because of the continuum of soliton pair states, which decrease in energy from E_g to $(2/\pi)E_g$ as a function of $S\bar{S}$ separation, Eqn. 2 can be *simultaneously* resonant at 3ω and at 2ω :⁴

$$\omega \rightarrow E_g/3 \quad (3\text{-photon resonance to the e-h pair continuum})$$

$$\omega \rightarrow E_g/\pi \quad (2\text{-photon resonance to the } S\bar{S} \text{ pair continuum})$$

Consequently, for conducting polymers with a degenerate ground state, $\chi^{(3)}(-3\omega;\omega,\omega,\omega)$ will be significantly enhanced by the neutral $S\bar{S}$ intermediate A_g state mechanism.

Calculations of Eqn.2 have been carried out using the neutral soliton pair A_g intermediate states.⁴ The ratio of the nonresonant prefactors defines the relative magnitudes of the rigid band contribution, $|\chi^{(3)}_{RB}|$ and the contribution from the neutral $S\bar{S}$ intermediate A_g state mechanism, $|\chi^{(3)}_{S\bar{S}}|$

$$|\chi^{(3)}_{S\bar{S}}| / |\chi^{(3)}_{RB}| = (\pi/2)\rho_s[\pi^2\xi_0/a]$$

where $\xi_0/a \approx 7$ is the half-width of the soliton measured in units of the carbon-carbon distance along the chain, and ρ_s is the density of solitons in the ground state as a result of quantum lattice fluctuations (nonlinear zero point motion). The magnitude of the nonlinear Franck-Condon factor was estimated from the 15% reduction in the bond-alternation compared with that calculated in the classical lattice approximation,¹⁵ due to nonlinear zero-point motion; $\rho_s \approx 0.025$.⁴ Substituting into Eqn 10 yields approximately 3 for the ratio.¹⁶ The $S\bar{S}$ intermediate state mechanism dominates *even off resonance* because the electronic enhancement factor, $(\pi/2)[\pi^2\xi_0/a] \approx 110$ is only partially offset by the nonlinear Franck-Condon overlap factor, $\rho_s \approx 0.025$. In addition, the contribution from the mechanism involving neutral soliton A_g intermediate states is further enhanced by the simultaneous 2- and 3-photon resonance (see Eqn. 3)⁴.

Since soliton pair confinement in a backbone structure with nondegenerate ground state (such as the *cis*-isomer of polyacetylene) limits the $S\bar{S}$ pair separation,¹ lifting the ground state

degeneracy is expected to quench the NLO mechanism arising from neutral soliton A_g intermediate states. This is qualitatively consistent with the data from *cis*-(CH) $_x$; the results in Figure 1 demonstrate that the nonresonant values of $\chi^{(3)}(3\omega)|_{cis}$ (dashed curve) are significantly smaller than $\chi^{(3)}(3\omega)|_{trans}$ (dot-dashed curve).

For *trans*-(CH) $_x$, the calculated curves are in agreement with the general frequency dependence of the $\chi^{(3)}(3\omega)$ data. The experimental results are, therefore, consistent with the simultaneous 2- and 3-photon resonance predicted by Eqn 3. The absolute magnitude of the calculated curve is of the correct order of magnitude, provided that prior to separation into a neutral soliton pair, Coulomb correlations bring the $2A_g$ state down in energy, close to the $1B_u$ state. A detailed comparison of the calculated curves (for various values of the Coulomb correlation parameter and the lifetime of the neutral soliton A_g state lifetime) with the data will be presented in a subsequent publication.

III. Conclusion

In conclusion, for *trans*-polyacetylene, $\chi^{(3)}(3\omega) \geq 10^{-8} - 10^{-7}$ esu for $\hbar\omega < E_g$. Since disorder localizes the π -electrons and thereby reduces the magnitude of $\chi^{(3)}$, high quality structurally ordered polymers are required to achieve the high performance values needed for use in photonics. The *cis/trans* comparison, and the general agreement of the calculated curves with the experimental results for *trans*-(CH) $_x$, imply that nonlinear zero-point motion enables the dominant contribution to $\chi^{(3)}(3\omega)$ via the correlated neutral soliton pair A_g intermediate state in conjugated polymers with degenerate ground state.

References:

1. A.J. Heeger, et al, Rev. Mod. Phys. **60**, 781 (1988).
2. G.P. Agrawal et al., Phys. Rev. **B17**, 776 (1978).
- 3.. R. Loudon, The Quantum Theory of Light (Clarendon Press, Oxford, 1983).
4. T. W. Hagler and A.J. Heeger, Chem. Phys. Lett. **189**, 333 (1992).
5. a. M. Sinclair, D. Moses, K. Akagi and A.J. Heeger, Phys. Rev. **B38**, 10724 (1988).
b. M. Sinclair, D. Moses, A.J. Heeger, J. Yu and W.P. Su, Proceedings of Nobel Symposium 73, Physica Scripta, **T27**, 144 (1989).
6. C. Halvorson et al, Proceedings of the Snowbird Conf.: "Optical Probes of Conjugated Polymers"; Synth. Met. (in press).
7. W.S. Fann, et al., Phys. Rev. Lett. **62**, 1492 (1989).
8. H. Shirakawa and S. Ikeda, Synth. Met. **1**, 175 (1979/1980)
9. a. B. Buchalter and G.R. Meredith, Appl. Optics, **21**(17), 3221 (1988)
b. I. H. Malitson, J. Opt. Soc. Am. **55**(10), 1205 (1965)
- 10 J. Jerphagnon, and S.K. Kurtz, J. Appl. Phys. **41**(4) 1667 (1970)
11. a.C. DeMelo and R. Silbey, Chem. Phys. Lett **140**, 537 (1987); J. Chem. Phys. **88**, 2567 (1988).
b.Z. Soos and S. Ramesesha, J. Chem. Phys. **90**, 1067 (1989); Chem. Phys. Lett. **153**, 171 (1988).
c G. Hurst et alJ. Chem Phys. **89**, 385 (1988).
d. J. R. Heflin et al., Phys. Rev. **B38**, 1573 (1988).
12. D. W. Hone and C. Singh, Phys. Rev. B (in press).
13. S. Kivelson and A.J. Heeger, Synth. Met. Synth.Met. **22**, 371 (1987).
14. Y. Cao, P. Smith, and A.J. Heeger, Polymer, **32**, 1210 (1991).
15. a. W.P. Su. Sol. St. Commun. **42**, 497 (1982).
b. E. Fradkin and J. E. Hirsch, Phys. Rev. **B27**, 1680 (1983).
16. The ratio, $\chi^{(3)}_{ssl} / \chi^{(3)}_{RB}$ (see Eqn 10), is a factor of 2π smaller than given in reference 4.

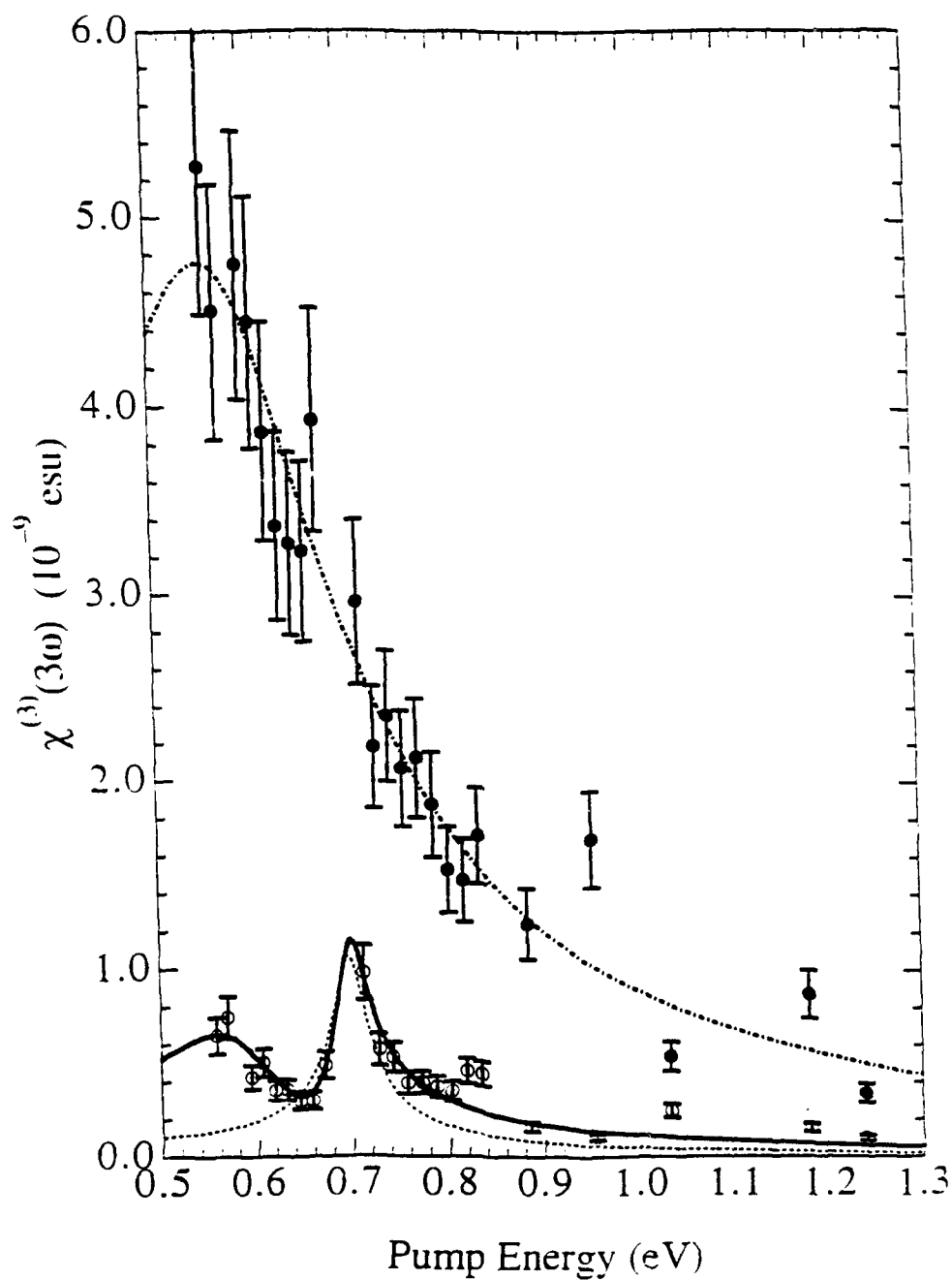


Figure 1: $\chi^{(3)}(3\omega)$ results obtained from THG measurements on "*cis*"- (open circles) and *trans*-(CH)_x (solid points); the solid curve represents the fit to Eqn 1 with $E_g(\text{cis})=2.09$ eV and $E_g(\text{trans})=1.72$ eV. The dashed and dot-dashed curves represent pure *cis*-(CH)_x and *trans*-(CH)_x, respectively.

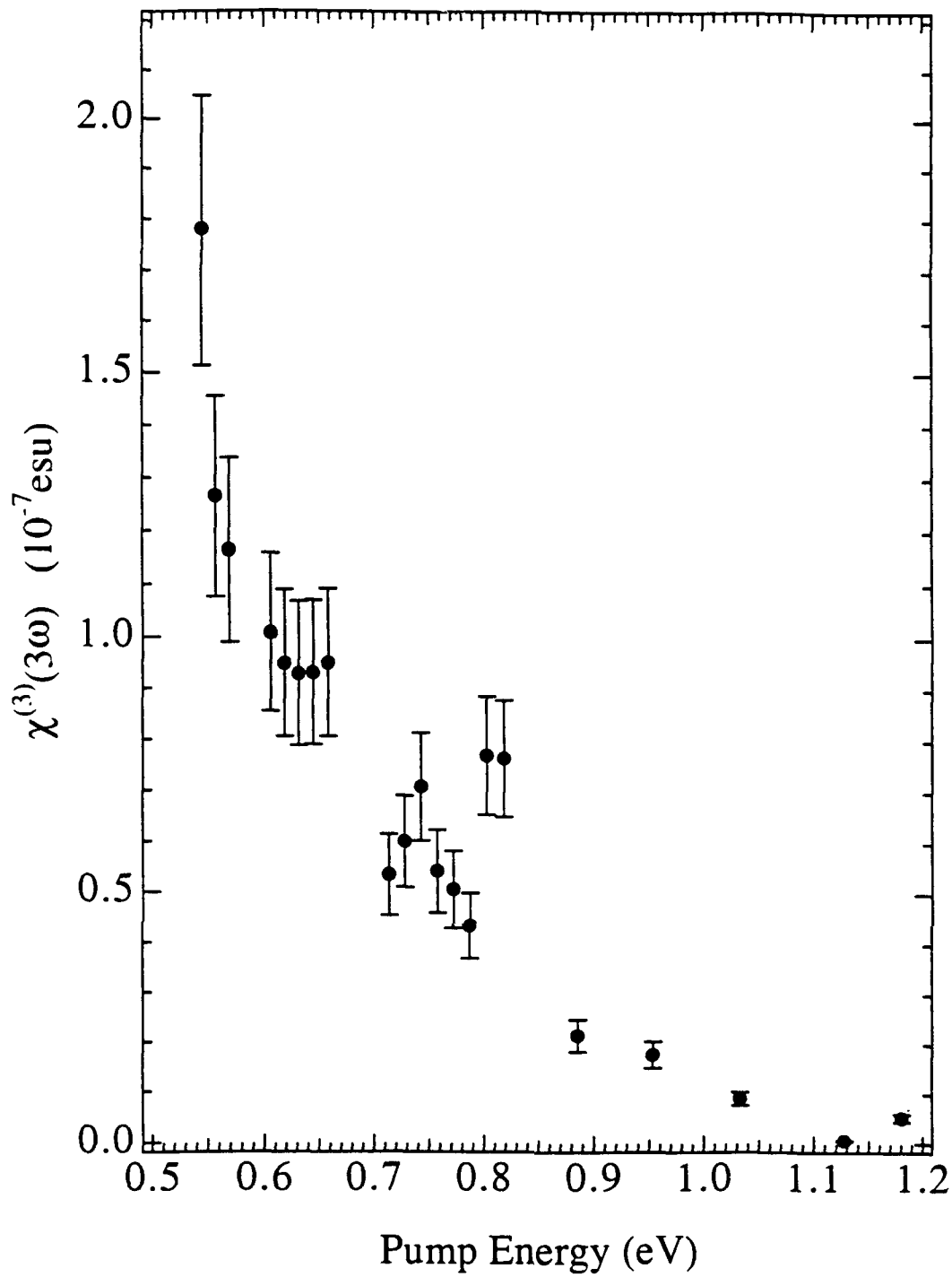


Figure 2: $\chi^{(3)}_{||}(3\omega)$ for an oriented sample of *trans*-(CH)_x (draw ratio 10); both the ω and 3ω beams are polarized parallel to the orientation direction.